

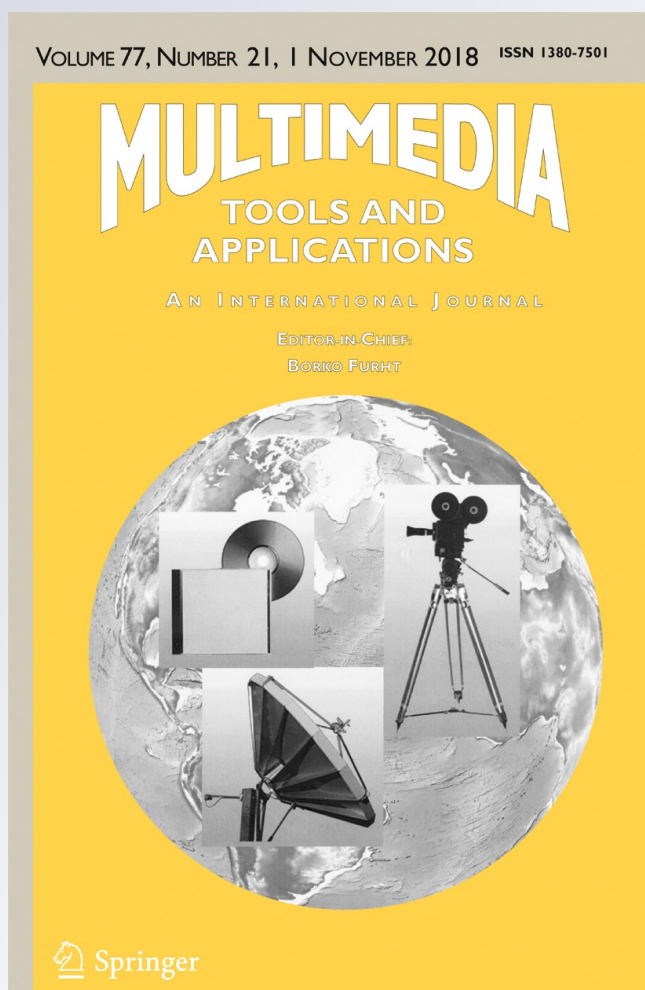
*A novel reversible data hiding scheme  
with two-dimensional histogram shifting  
mechanism*

**Phuoc-Hung Vo, Thai-Son Nguyen,  
Van-Thanh Huynh & Thanh-Nghi Do**

**Multimedia Tools and Applications**  
An International Journal

ISSN 1380-7501  
Volume 77  
Number 21


Multimed Tools Appl (2018)  
77:28777-28797  
DOI 10.1007/s11042-018-5991-8



**Your article is protected by copyright and all rights are held exclusively by Springer Science+Business Media, LLC, part of Springer Nature. This e-offprint is for personal use only and shall not be self-archived in electronic repositories. If you wish to self-archive your article, please use the accepted manuscript version for posting on your own website. You may further deposit the accepted manuscript version in any repository, provided it is only made publicly available 12 months after official publication or later and provided acknowledgement is given to the original source of publication and a link is inserted to the published article on Springer's website. The link must be accompanied by the following text: "The final publication is available at [link.springer.com](http://link.springer.com)".**



# A novel reversible data hiding scheme with two-dimensional histogram shifting mechanism

Phuoc-Hung Vo<sup>1,2</sup> · Thai-Son Nguyen<sup>1</sup>  · Van-Thanh Huynh<sup>1</sup> · Thanh-Nghi Do<sup>2</sup>

Received: 23 October 2017 / Revised: 21 March 2018 / Accepted: 9 April 2018 /  
Published online: 5 May 2018  
© Springer Science+Business Media, LLC, part of Springer Nature 2018

**Abstract** In this paper, we propose a novel reversible data hiding technique based on two-dimensional histogram shifting for quantized discrete cosine transformation coefficients (QDCT). In the proposed scheme, a two-dimensional histogram is constructed by QDCT coefficients blocks with the size of  $8 \times 8$  of the left image and the right image. Once most of the QDCT coefficients are located at the top-right corner of the two-dimensional histogram, the QDCT coefficients are selected for embedding data to achieve high embedding capacity. In the embedding procedure, the three main steps, i.e., expanding, shifting, and embedding, are only used for QDCT coefficients in this corner not only to gain embedding capacity, but also to maintain good visual quality of stego images. The experimental results demonstrated that the proposed scheme is superior to the previous schemes in terms of embedding capacity and image quality.

**Keywords** Reversible · Data hiding · DCT · 2D histogram shifting · Stereo image · 3D image

---

✉ Thai-Son Nguyen  
thaison@tvu.edu.vn

Phuoc-Hung Vo  
hungvo@tvu.edu.vn

Van-Thanh Huynh  
hvthanh@tvu.edu.vn

Thanh-Nghi Do  
dtngchi@cit.ctu.edu.vn

<sup>1</sup> School of Engineering and Technology, Tra Vinh University, Tra Vinh City, Tra Vinh Province, Vietnam

<sup>2</sup> College of Information Technology, Can Tho University, Can Tho 92100, Vietnam

## 1 Introduction

In recent years, with the spread of high-technology equipment with dual-cameras, an increasing amount of images are created as so-called stereo images, which present the illusion of 3D depth images [22]. In addition, with the explosive growth of network and rapid communication techniques, an enormous amount of digital information is transmitted via the Internet every second. However, such transmitted information is highly sensitive, such as medical patient detail information. Thus, this data attracts the attention of malicious attackers. Therefore, protecting the security of such information is of considerable concern to many researchers. For decades, the researchers have tried to propose schemes to avoid the attention of malicious attackers. Therefore, the security of the transmitted digital information is guaranteed. Several schemes that have been proposed can be divided into two different techniques: cryptography and steganography (data hiding). In the cryptography technique, the information is transformed into meaningless values by well-known encryption schemes, such as DES [19], AES [20], and RSA [21], and then are sent to the receiver. Hence, this technique increases the curiosity of unauthorized users. Unlike cryptography, data hiding techniques are the science of embedding information into cover digital multimedia, such as images, video, and audio. The cover image after being embedded with secret data, called as stego-image, is still in a meaningful format. Therefore, data hiding techniques can avoid attracting attackers' attention.

Data hiding systems for images can be classified into two various categories, i.e., spatial domain and frequency domain. In the spatial domain, the secret messages are embedded directly into the pixel values of the cover images [2, 4, 7, 12, 15, 16, 18, 23]. The most popular data hiding technique in this category is based on least significant bit (LSB) of pixels for holding the secret data. In 2003, Tian [23] proposed a reversible data hiding scheme based on different expansion (DE) of two pixels in the cover image to embed secret bits. Reversible data hiding (RDH), also referred to as lossless or invertible data hiding, can recover the original image without any distortion after the hidden data has been extracted. DE is one of the most important techniques used for reversible data hiding. However, during embedding in Tian's scheme, to prevent overflow and underflow problems, a location map is formed to distinguish between the expandable and changeable difference values. In 2017, Parah et al. [16] proposed a new reversible and high capacity data hiding technique for E-healthcare applications on which the Electronic Patient Record was embedded only in non-seed pixels of blocks. In the frequency domain [3, 6, 8, 11, 13, 14, 17, 25, 26], the cover image is transformed to coefficients by using transformation techniques, such as discrete cosine transformation (DCT) or discrete wavelet transformation (DWT). Then, these coefficients are used to carry the secret data. For instance, Chang et al.'s scheme [3] utilized the medium frequency coefficients of the DCT algorithm to embed the secret data. Owing to the importance being given to medical image, Parah et al. [13] proposed a robust watermarking technique for medical image based on DWT. The medical image is transformed to subbands and watermark is only embedded into LH subband.

Most of these RDH algorithms are proposed only for 2D images [2–4, 6–8, 11–18, 23, 25, 26]. Recently, stereoscopy techniques have been used to take pictures with the perception of 3D depth from a pair of given 2D images, so-called stereo-images. Patrizio Campisi [1] proposed an object-oriented scheme for watermarking stereo images. In this scheme, a depth map is extracted from a pair of stereo images and then the watermark embedding is performed in the wavelet domain using the quantization index modulation scheme. In 2014, Luo et al. [9] proposed a stereo image watermarking scheme for authentication with self-recovery capability

using inter-view reference sharing. However, all the above-mentioned schemes are generally referred to as irreversible data hiding schemes so that they are not suitable for medical, military, or forensic application. For instance, in the health service, the patient information is hidden in the X-ray image. Both of them are so important to the receiver, so they must be recovered at the receiving side. Therefore, there is a need to have reversible data hiding schemes [10].

To overcome these issues, in 2015, Yang et al. [26] proposed reversible DCT-based data hiding in stereo images. The scheme encoded each 3-bit secret into two integer digits in intervals  $[-1, 1]$  and then embedded them into the difference of QDCT coefficients. In this scheme, the cover image can be restored to its original version after extracting the secret message. However, the embedding capacity is rather limited, smaller than 0.26 bpp for a threshold of 30, as shown in the experimental results, since the scheme depended on number of different value zeros between the QDCT coefficients in the left and the right images. Then, the histogram shifting algorithm is utilized for hiding the secret data into such different values to obtain reversibility. This means that most of the different values must be modified during the embedding process. Consequently, the obtained stego-image is significantly distorted.

To further improve the embedding capacity and maintain the good visual quality of stego-images, a novel reversible data hiding scheme is proposed. In the proposed scheme, a two-dimensional (2D) histogram of QDCT coefficients is constructed. Then, the histogram is divided into four directions. However, only one direction of the histogram is selected and implemented for embedding secret data to obtain higher embedding capacity while maintaining the minimum distortion of the stego-image. The rest of the paper is presented as follows. In Section 2, we briefly review the DCT transformation and Yang et al.'s scheme. We propose a high capacity RDH scheme using 2D histogram shifting and illustrate this scheme in Section 3. Experimental results are demonstrated in Section 4, and the conclusion is presented in Section 5.

## 2 Related works

### 2.1 Discrete cosine transform and quantization table

DCT is an important technique for image transformation and is applied in numerous well-known scientific and engineering applications, such as JPEG encoding. Figure 1 shows the flowchart of the JPEG encoder.

The input image is first partitioned into non-overlapping  $8 \times 8$  blocks, then each block is transformed into the DCT domain using Eq. (1).

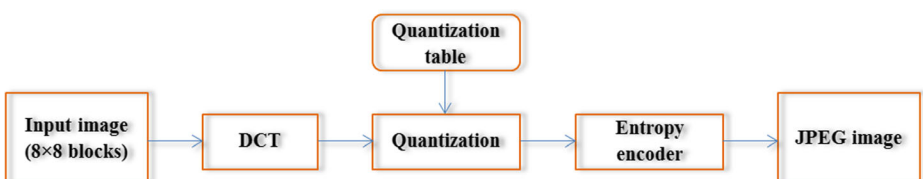


**Fig. 1** The flowchart of the JPEG encoder

$$F(u, v) = \frac{c(u)c(v)}{4} \sum_{x=1}^8 \sum_{y=1}^8 f(x, y) \cos\left(\frac{(2x-1)u\pi}{16}\right) \cos\left(\frac{(2y-1)v\pi}{16}\right) \tag{1}$$

where  $c(e) = \begin{cases} \frac{1}{\sqrt{2}}, & \text{if } e = 0 \\ 1, & \text{otherwise.} \end{cases}$

$F(u, v)$  with  $u$  and  $v$  running from 1 to 8 is the DCT coefficient at the coordinate  $(u, v)$  and  $f(x, y)$  means pixel value at the coordinate  $(x, y)$ , which is a specific zigzag order of the transform coefficient levels from the lowest to highest frequency to generate two components, i.e., DC and AC. Then, in the quantization stage, DCT coefficients are quantized by using Eq. (2) with a quantization table having 64 entries formed to the  $8 \times 8$  matrix.

$$D(u, v) = \text{round}\left(\frac{F(u, v)}{Q(u, v)}\right) \tag{2}$$

where  $Q(u, v)$  is corresponding value in the quantization table and  $D(u, v)$  is QDCT coefficients. Figure 2 shows the standard quantization table with the quality factor  $QF$  equal to 50 [25].

### 2.2 Yang and Chen’s scheme

Stereo images have a pair of images, the left image and the right image. These two images are the same size and are very similar. According to this property, in 2015, Yang and Chen [26] proposed reversible DCT-based data hiding in stereo images by determining the most similar block pairs in the left and the right images. Then, the QDCT coefficients of the most similar block pairs are modified to embed the secret data. Their scheme is divided into two main procedures: embedding and extracting. In the embedding procedure, each image is first partitioned into  $8 \times 8$  blocks. Then, these blocks are transformed and quantized into DCT domain. The QDCT coefficients of each block are categorized into three areas: (1) The searching area contains lower frequency QDCT coefficients  $C(u, v)$  (where  $u, v$  is from 1 to

<b>16</b>	<b>11</b>	<b>10</b>	<b>16</b>	<b>24</b>	<b>40</b>	<b>51</b>	<b>61</b>
<b>12</b>	<b>12</b>	<b>14</b>	<b>19</b>	<b>26</b>	<b>58</b>	<b>60</b>	<b>55</b>
<b>14</b>	<b>13</b>	<b>16</b>	<b>24</b>	<b>40</b>	<b>57</b>	<b>69</b>	<b>56</b>
<b>14</b>	<b>17</b>	<b>22</b>	<b>29</b>	<b>51</b>	<b>87</b>	<b>80</b>	<b>62</b>
<b>18</b>	<b>22</b>	<b>37</b>	<b>56</b>	<b>68</b>	<b>109</b>	<b>103</b>	<b>77</b>
<b>24</b>	<b>35</b>	<b>55</b>	<b>64</b>	<b>81</b>	<b>104</b>	<b>113</b>	<b>92</b>
<b>49</b>	<b>64</b>	<b>78</b>	<b>87</b>	<b>103</b>	<b>121</b>	<b>120</b>	<b>101</b>
<b>72</b>	<b>92</b>	<b>95</b>	<b>98</b>	<b>112</b>	<b>100</b>	<b>103</b>	<b>99</b>

Fig. 2 Standard quantization table  $Q_{50}$

8 and  $u + v \leq 4$ ); (2) The embedding area includes middle frequency QDCT coefficients  $C(u, v)$  (where  $7 \leq u + v \leq 9$ ); (3) The non-used area contains the rest of non-used coefficients. Next, for each block in the left image, the similar block is determined in the right image based on the different values of the QDCT coefficients of these two blocks in the searching area. Before embedding the secret data, the different value  $Dif B(u, v)$  of the QDCT coefficients in the embedding area between  $B^L$  and  $B^R$  are calculated by the following equation:

$$Dif B(u, v) = C_{B^L}(u, v) - C_{B^R}(u, v), 7 \leq u + v \leq 9 \tag{3}$$

If  $Dif B(u, v)$  which is equal to value of zero is used to embed the secret digit  $z \in [-1, 1]$  by using Eq. (4).

$$Dif' B(u, v) = \begin{cases} Dif B(u, v) + 1, & \text{if } Dif B(u, v) > 0 \\ z, & \text{if } Dif B(u, v) = 0 \\ Dif B(u, v) - 1, & \text{if } Dif B(u, v) < 0 \end{cases} \tag{4}$$

Then, the new different value  $Dif' B(u, v)$ , is used to update the frequency QDCT coefficients into the left and the right block of stereo image. By using above steps, the secret data is embedded into the stereo image. However, in this scheme, to embed secret data, most of the QDCT coefficients in the embedding area of the left and the right images will change values, which has a significant effect on the visual quality of the stego stereo images. In addition, based on 1D histogram shifting algorithm for hiding, the embedding capacity of Yang and Chen's scheme is limited by the number of different values zero.

### 3 The proposed scheme

As mentioned in Section 2, the shortcomings in terms of embedding capacity and visual quality of stego-images in Yang et al.'s scheme is identified. The scheme depends on the occurrence of zero difference values of the QDCT coefficients pairs and the one-dimensional histogram shifting schemes for information hiding. To increase embedding capacity and visual quality for the stego stereo images, we propose a new scheme based on building a 2D histogram shift. The proposed scheme reduces the modification of the QDCT coefficient values and the secret data directly embedded in each QDCT coefficient pair. The scheme is made of two procedures: embedding and extracting.

#### 3.1 Embedding process

Based on the property of the stereo image, having many similar block pairs on the left and right image, the novel RDH scheme for stereo image is proposed. Figure 3 shows an example of a stereo image with the left image (Fig. 3a) and right image (Fig. 3b). Inspired by scheme [3], in the proposed scheme, the QDCT coefficients are also divided into three different areas, namely (i) searching; (ii) embedding, and (iii) non-used areas, for data embedding strategy. Specifically, each left and right images are partitioned into non-overlapping  $8 \times 8$  blocks in the frequency QDCT domain. Next, the similar block pair is determined based on the searching area and the defined threshold  $T$ . Then, the secret data will be embedded in the embedding area of those determined similar block pairs. The flowchart of the embedding procedure is shown in Fig. 4.

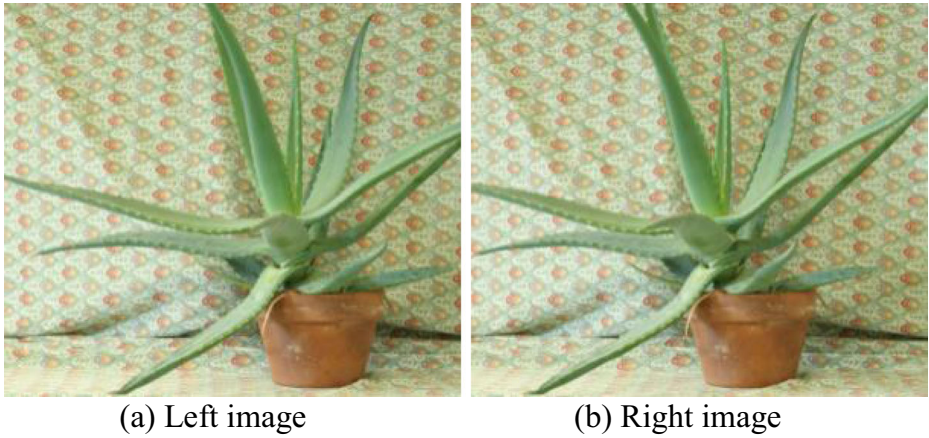


**Fig. 3** An example of stereo image pair. **a** Left image, **b** Right image

### 3.1.1 Similar block searching

Each image is partitioned into blocks with a size of  $8 \times 8$  in the DCT domain and classified into three areas demonstrated in Fig. 5. With each block  $B^L$  in the left image, the most similar block  $B^R$  in the right image is searched in the searching area by Eq. (5).

Two blocks are labeled as the most similar block pair when the smallest different value is obtained. Those found similar block pairs are used for embedding secret data into the embedding area of the found similar block pair.

$$Dist(B) = \sum_{u,v=1}^{u+v \leq 4} [C_{B^L}(u,v) - C_{B^R}(u,v)]^2 \tag{5}$$

where  $C(u, v)$  stands for the QDCT coefficient at  $(u, v)$  coordinate in the block.

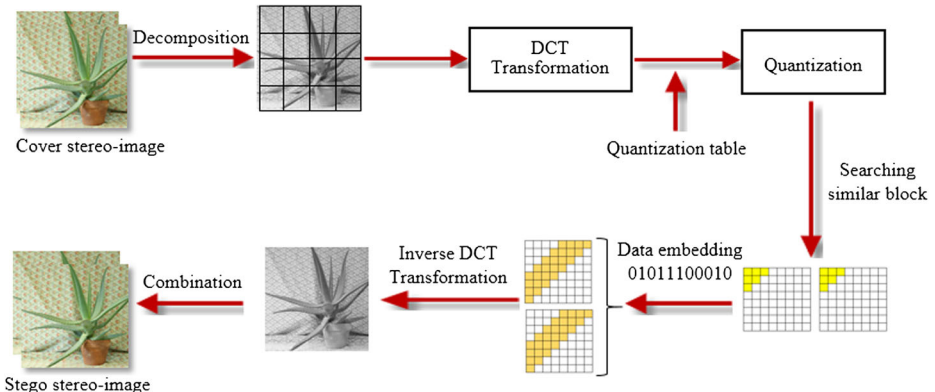


**Fig. 4** The flowchart of the proposed embedding process in stereo images



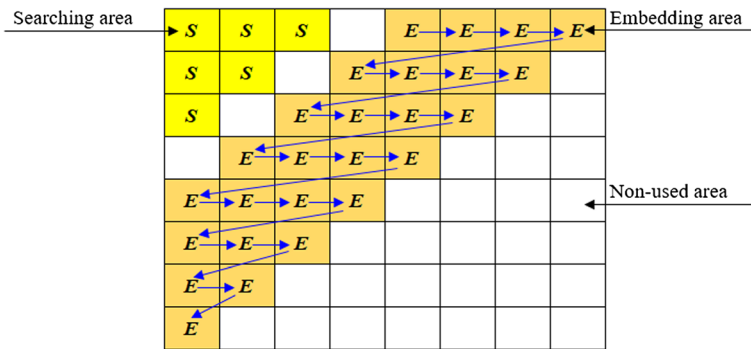


Fig. 5 Three areas of an 8×8 block in DCT domain (S: Searching area, E: Embedding area, blank: non-used area)

### 3.1.2 2D histogram shifting based lossless Data embedding

Based on 1D histogram shifting algorithm for hiding, the embedding capacity of Yang and Chen’s scheme is limited while the visual image quality is not satisfied. In this subsection, a 2D histogram is defined. The 2D histogram denoted as  $h(x, y)$ , where  $x$  and  $y$  are the frequencies of two feature values, belong to the QDCT left and right block. Taking advantage of the similarities of the left and right images in the stereo images, 2D histogram shifting is used for embedding data bits into cover stereo-images, we explored the coefficients of QDCT located in the embedding area (i.e.,  $6 \leq u + v \leq 9$ ) quietly approaching zero or positive value. Based on our scheme, the larger the number of zero coefficients is, the greater embedding capacity is obtained. Moreover, the trend of these coefficients commonly gathers at the top-right corner of the histogram (i.e., NE direction). Thus, the 2D shifting and data embedding are conducted at this corner (see Fig. 6) to achieve high embedding capacity while maintaining the good stego-stereo image quality as shown in the experimental results.

Assume that the secret data-bit is  $s$ . The data-bit embedding order is listed in Fig. 5. The embedding procedure could be described as following steps:

Input: The quantization left block  $B_Q^L$ , the most similar quantization right block  $B_Q^R$  and secret bit  $s$ .

Output: The stego quantization left block  $B_Q^{L'}$  and right block  $B_Q^{R'}$ .

Step 1. Expanding:

With each block pair  $B_Q^L$  and  $B_Q^R$ , QDCT coefficients expand in the embedding area by following Eq. (6),

$$\begin{cases} B_Q^{L'}(u, v) = B_Q^L(u, v) + 1 \\ B_Q^{R'}(u, v) = B_Q^R(u, v) \end{cases}, \text{ if } \begin{cases} B_Q^L(u, v) > B_Q^R(u, v) \text{ and} \\ \lfloor B_Q^L(u, v) \rfloor > 1 \end{cases} \quad (6)$$

$$\begin{cases} B_Q^{L'}(u, v) = B_Q^L(u, v) \\ B_Q^{R'}(u, v) = B_Q^R(u, v) + 1 \end{cases}, \text{ if } \begin{cases} B_Q^R(u, v) > B_Q^L(u, v) \text{ and} \\ \lfloor B_Q^R(u, v) \rfloor > 1 \end{cases}$$

where  $\lfloor \cdot \rfloor = \text{round}(\cdot)$

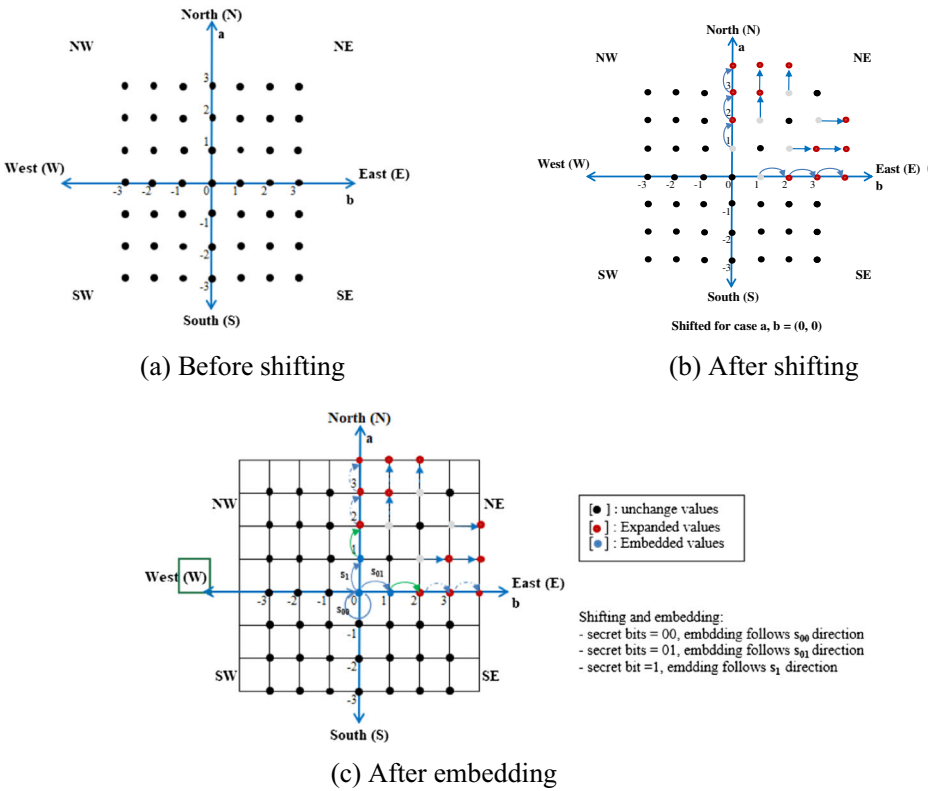


**Fig. 6** The 2D histogram used in the proposed scheme

**Step 2. Shifting and Embedding:**

Step 2.1 if  $[B_Q^L(u, v)] = 0$  and  $[B_Q^R(u, v)] = 0$ , the secret data  $s$  is embedded by Eq. (7),

$$\begin{cases} B_Q^{L'}(u, v) = B_Q^L(u, v) \text{ and } B_Q^{R'}(u, v) = B_Q^R(u, v), & \text{if } s = 00 \\ B_Q^{L'}(u, v) = B_Q^L(u, v) \text{ and } B_Q^{R'}(u, v) = B_Q^R(u, v) + 1, & \text{if } s = 01 \\ B_Q^{L'}(u, v) = B_Q^L(u, v) + 1 \text{ and } B_Q^{R'}(u, v) = B_Q^R(u, v), & \text{if } s = 1 \end{cases} \quad (7)$$

Step 2.2 if  $[B_Q^L(u, v)] = 0$  and  $[B_Q^R(u, v)] = 1$ , the secret data  $s$  is embedded by Eq. (8),

$$\begin{cases} B_Q^{L'}(u, v) = B_Q^L(u, v) \text{ and } B_Q^{R'}(u, v) = B_Q^R(u, v) + 1, & \text{if } s = 0 \\ B_Q^{L'}(u, v) = B_Q^L(u, v) + 1 \text{ and } B_Q^{R'}(u, v) = B_Q^R(u, v) + 1, & \text{if } s = 1 \end{cases} \quad (8)$$

Step 2.3 if  $[B_Q^L(u, v)] = 1$  and  $[B_Q^R(u, v)] = 0$ , the secret data  $s$  is embedded by Eq. (9),

$$\begin{cases} B_Q^{L'}(u, v) = B_Q^L(u, v) + 1 \text{ and } B_Q^{R'}(u, v) = B_Q^R(u, v), & \text{if } s = 0 \\ B_Q^{L'}(u, v) = B_Q^L(u, v) + 1 \text{ and } B_Q^{R'}(u, v) = B_Q^R(u, v) + 1, & \text{if } s = 1 \end{cases} \quad (9)$$

3.1.3 For better explanation, taking an example of embedding

An example is given to depict the presented data embedding process clearly. For a stereo-image shown as in the Fig. 3,

1. With the threshold  $T = 5$  and quantization table  $Q_{50}$  these two blocks  $B_{15}^L$  and  $B_{13}^R$  are found as the most similar block pair since the smallest different value of QDCT coefficients shown as in Fig. 7e and f is  $Dist(B) = 3.8$ , and this value is smaller than the threshold  $T$ .
2. Figure 8a and b show a 2D shifting algorithm applied to the embedding area of two DCT quantization blocks  $B_Q^L$  and  $B_Q^R$ .
3. Assume secret bits  $s = 10100100101011100110010001000111101$ . The embedding process 33-bit  $s$  in the embedding area is executed almost continuously in which two parameters  $u$  and  $v$  indexing row and column, respectively are running from 1 to 8 such that  $(6 \leq u + v \leq 9)$  distributed as following Table 1:

104	102	103	107	123	146	152	152
101	104	102	105	106	112	121	144
96	95	100	105	102	104	132	132
128	101	90	97	109	106	106	106
137	113	90	94	111	105	106	113
112	107	113	115	118	119	119	125
143	148	148	146	148	151	153	156
166	153	141	133	134	139	140	140

(a) Original left block  $B_{15}^L$

95	106	105	103	108	132	151	152
95	103	105	103	109	109	115	128
101	94	98	101	107	102	110	138
139	122	95	89	105	107	106	107
117	137	99	90	102	108	106	108
110	111	108	114	118	117	120	124
142	147	147	146	146	148	152	154
167	163	146	135	133	138	144	144

(b) Original right block  $B_{13}^R$

966.125	-0.644	38.6056	13.0334	10.875	-0.0554	0.10961	2.14907
-78.008	-52.711	5.30383	-5.3634	-0.3435	1.82119	-1.3783	-1.0233
88.9735	-22.361	-2.1187	-11.196	-15.921	-1.2373	3.78661	-4.2213
0.50376	-18.01	-8.3074	6.41316	-1.5465	-6.0829	4.5762	-1.4983
-4.375	21.3621	13.6416	30.4382	4.375	-1.5826	1.2497	1.16635
30.2882	-15.065	-12.499	3.25806	-6.6946	5.12631	-0.1919	1.5359
-19.4	-12.87	-3.9634	-2.8844	-5.4468	8.53898	-0.8813	2.55887
19.2475	-7.1823	5.70775	-1.3671	-3.4257	0.70035	-5.8354	1.67128

(c) DCT transform left block  $B_D^L$

960.125	-25.835	42.9448	2.31462	-2.625	-14.008	-5.7467	-1.3832
-90.967	-46.708	3.78156	-7.5849	1.88569	-0.5317	3.18287	1.56261
81.5496	-27.927	-4.6239	-15.41	-7.8714	11.8398	3.04182	0.65647
-9.1637	-24.959	-10.187	-1.3043	-13.783	0.02935	-5.5786	-3.9634
4.625	24.4402	24.8307	18.2542	-15.125	-3.7706	-6.3615	-3.2681
31.1969	-13.686	1.47936	4.81704	3.54091	7.91178	3.4193	2.13333
-19.031	-16.374	2.79182	-4.5863	7.4547	4.80308	2.62392	0.41951
12.4624	-10.65	0.77476	-10.56	-4.3165	-5.4354	-1.7247	-2.8998

(d) DCT transform right block  $B_D^R$

60.3828	-3.6949	3.86056	0.81459	0.45313	-0.0014	0.00215	0.03523
-6.5007	-4.3926	0.37884	-0.2823	-0.0132	0.0314	-0.023	-0.0186
6.35525	-1.7201	-0.1324	-0.4665	-0.398	-0.0217	0.05488	-0.0754
0.03598	-1.0594	-0.3776	0.22114	-0.0303	-0.0699	0.0572	-0.0242
-0.2431	0.97101	0.36889	0.54354	0.06434	-0.0145	0.01213	0.01515
1.26201	-0.4304	-0.2273	0.05091	-0.0826	0.04929	-0.0017	0.01669
-0.3959	-0.2011	-0.0508	-0.0332	-0.0529	0.07057	-0.0073	0.02534
0.26733	-0.0781	0.06008	-0.014	-0.0306	0.007	-0.0567	0.01688

(e) DCT quantization left block  $B_Q^L$  with  $Q_{50}$

60.0078	-2.3486	4.29448	0.14466	-0.1094	-0.3502	-0.1127	-0.0227
-7.5805	-3.8923	0.26868	-0.3992	0.07253	-0.0092	0.05305	0.02841
5.82497	-2.1482	-0.289	-0.6421	-0.1968	0.20772	0.04408	0.01172
-0.6546	-1.4682	-0.463	-0.045	-0.2702	0.00034	-0.0697	-0.0639
0.25694	1.11092	0.6711	0.32597	-0.2224	-0.0346	-0.0618	-0.0424
1.29987	-0.391	0.0269	0.07527	0.04371	0.07607	0.03026	0.02319
-0.3884	-0.2558	0.03579	-0.0527	0.07238	0.03969	0.02187	0.00415
0.17309	-0.1158	0.00816	-0.1078	-0.0385	-0.0544	-0.0167	-0.0293

(f) DCT quantization right block  $B_Q^R$  with  $Q_{50}$

Fig. 7 Example for searching similar block

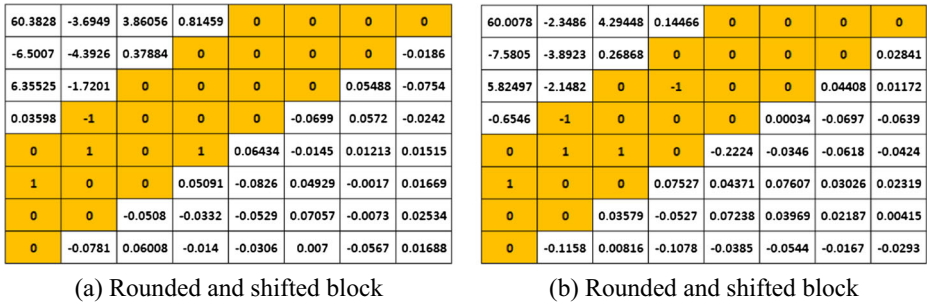


Fig. 8 Example for 2D histogram shifting

4. Finally, two stego-blocks  $B_Q^L$  and  $B_Q^R$  are obtained as Fig. 9.

### 3.2 Extracting process

The extracting process is like the embedding process. First, each stego-stereo image is divided into  $8 \times 8$  pixels non-overlap blocks. Second, for each block, the left stego-image  $sB^L$  and the most similar block in the right stego-image  $sB^R$  are found through Eq. (5). Lastly, the secret bit is extracted from the similar quantization block pairs. The details are given as the following steps:

Input: Stego-stereo image.  
 Output: Original stereo image and secret bits.

- Step 1. Divide each the stego-image into  $8 \times 8$  blocks
- Step 2. For each quantization block  $sB_Q^L$  in left stego image, and the most similar block  $sB_Q^R$  in the right stego-image, which is evaluated by Eq. (5) for DCT quantization coefficients in the searching area, the cover stereo-image left block  $sB_Q^L$  and right block  $sB_Q^R$  are restored and the secret data is extracted. The process is as shown below:

Case 1-1: if  $[sB_Q^L(u, v)] = 0$  and  $[sB_Q^R(u, v)] = 0$  then set secret bits  $s = 00$  and restore  $sB_Q^L(u, v) = sB_Q^L(u, v), sB_Q^R(u, v) = sB_Q^R(u, v);$

Table 1 The embedding process 33-bit secret

Row	Embedded secret bits	Number of bit
1	1 01 00 1	6
2	00 1 01 01	7
3	1 01 1	4
4	00 1 00	5
5	01 0 0	4
6	01 1	3
7	1 1	2
8	01	2

60.3828	-3.6949	3.86056	0.81459	1.45313	-0.0014	0.00215	1.03523	60.0078	-2.3486	4.29448	0.14466	-0.1094	0.64979	-0.1127	-0.0227
-6.5007	-4.3926	0.37884	-0.2823	0.98679	0.0314	-0.023	-0.0186	-7.5805	-3.8923	0.26868	-0.3992	0.07253	0.99083	1.05303	0.02841
6.35525	-1.7201	0.86758	-0.4665	-0.398	0.97829	0.05488	-0.0754	5.82497	-2.1482	-0.289	-0.6421	0.80322	0.20772	0.04408	0.01172
0.03598	-1.0594	-0.3776	1.22114	-0.0303	-0.0699	0.0572	-0.0242	-0.6546	-1.4682	-0.463	-0.045	-0.2702	0.00034	-0.0697	-0.0639
-0.2431	0.97101	0.36869	1.54354	0.06434	-0.0145	0.01213	0.01515	1.25694	2.11092	1.6711	0.32597	-0.2224	-0.0346	-0.0618	-0.0424
1.26201	-0.4304	0.77275	0.05091	-0.0826	0.04929	-0.0017	0.01669	2.29987	0.60897	0.0269	0.07527	0.04371	0.07607	0.03026	0.02319
0.60407	0.79891	-0.0508	-0.0332	-0.0529	0.07057	-0.0073	0.02534	-0.3884	-0.2558	0.03579	-0.0527	0.07238	0.03969	0.02187	0.00415
0.26733	-0.0781	0.06008	-0.014	-0.0306	0.007	-0.0567	0.01688	1.17309	-0.1158	0.00816	-0.1078	-0.0385	-0.0544	-0.0167	-0.0293

(a) Embedded block  $B_Q^L$

(b) Embedded block  $B_Q^R$

Fig. 9 Example for embedding secret data

Case 1-2: if  $[sB_Q^L(u, v)] = 0$  and  $[sB_Q^R(u, v)] = 1$  then set secret bits  $s = 01$  and restore

$$sB_Q^L(u, v) = sB_Q^L(u, v), sB_Q^R(u, v) = sB_Q^R(u, v) - 1;$$

Case 1-3: if  $[sB_Q^L(u, v)] = 1$  and  $[sB_Q^R(u, v)] = 0$  then set secret bit  $s = 1$  and restore

$$sB_Q^L(u, v) = sB_Q^L(u, v) - 1, sB_Q^R(u, v) = sB_Q^R(u, v);$$

Case 2-1: if  $[sB_Q^L(u, v)] = 0$  and  $[sB_Q^R(u, v)] = 2$  then set secret bit  $s = 0$  and restore

$$sB_Q^L(u, v) = sB_Q^L(u, v), sB_Q^R(u, v) = sB_Q^R(u, v) - 1;$$

Case 2-2: if  $[sB_Q^L(u, v)] = 1$  and  $[sB_Q^R(u, v)] = 2$  then set secret bit  $s = 1$  and restore

$$sB_Q^L(u, v) = sB_Q^L(u, v) - 1, sB_Q^R(u, v) = sB_Q^R(u, v) - 1;$$

Case 3-1: if  $[sB_Q^L(u, v)] = 2$  and  $[sB_Q^R(u, v)] = 0$  then set secret bit  $s = 0$  and restore

$$sB_Q^L(u, v) = sB_Q^L(u, v) - 1, sB_Q^R(u, v) = sB_Q^R(u, v);$$

Case 3-2: if  $[sB_Q^L(u, v)] = 2$  and  $[sB_Q^R(u, v)] = 1$  then set secret bit  $s = 1$  and restore

$$sB_Q^L(u, v) = sB_Q^L(u, v) - 1, sB_Q^R(u, v) = sB_Q^R(u, v) - 1;$$

Case 4-1: if  $sB_Q^L(u, v) > sB_Q^R(u, v)$  and  $[sB_Q^L(u, v)] > 2$  then shift back and restore

$$sB_Q^L(u, v) = sB_Q^L(u, v) - 1, sB_Q^R(u, v) = sB_Q^R(u, v);$$

Case 4-2: if  $sB_Q^R(u, v) > sB_Q^L(u, v)$  and  $[sB_Q^R(u, v)] > 2$  then shift back and restore

$$sB_Q^L(u, v) = sB_Q^L(u, v), sB_Q^R(u, v) = sB_Q^R(u, v) - 1;$$

Step 3. Repeat Step 2 until all blocks are processed.

To make more clearly recovery process, an example is invoked in Fig. 10, which has been inherited by an example in the previous section.

## 4 Experimental results

In this section, we conducted various experiments to evaluate the performance of the proposed scheme. A test dataset from Middlebury [24] are used in our experimental results. This dataset

60.3828	-3.6949	3.86056	0.81459	1.45313	-0.0014	0.00215	1.03523
-6.5007	-4.3926	0.37884	-0.2823	0.98679	0.0314	-0.023	-0.0186
6.35525	-1.7201	0.86758	-0.4665	-0.398	0.97829	0.05488	-0.0754
0.03598	-1.0594	-0.3776	1.22114	-0.0303	-0.0699	0.0572	-0.0242
-0.2431	0.97101	0.36869	1.54354	0.06434	-0.0145	0.01213	0.01515
1.26201	-0.4304	0.77275	0.05091	-0.0826	0.04929	-0.0017	0.01669
0.60407	0.79891	-0.0508	-0.0332	-0.0529	0.07057	-0.0073	0.02534
0.26733	-0.0781	0.06008	-0.014	-0.0306	0.007	-0.0567	0.01688

(a) Stego-quantization left block  $sB_Q^L$

60.0078	-2.3486	4.29448	0.14466	-0.1094	0.64979	-0.1127	-0.0227
-7.5805	-3.8923	0.26868	-0.3992	0.07253	0.99083	1.05305	0.02841
5.82497	-2.1482	-0.289	-0.6421	0.80322	0.20772	0.04408	0.01172
-0.6546	-1.4682	-0.463	-0.045	-0.2702	0.00034	-0.0697	-0.0639
1.25694	2.11092	1.6711	0.32597	-0.2224	-0.0346	-0.0618	-0.0424
2.29987	0.60897	0.0269	0.07527	0.04371	0.07607	0.03026	0.02319
-0.3884	-0.2558	0.03579	-0.0527	0.07238	0.03969	0.02187	0.00415
1.17309	-0.1158	0.00816	-0.1078	-0.0385	-0.0544	-0.0167	-0.0293

(b) Stego-quantization right block  $sB_Q^R$

60.3906	-3.7025	3.86733	0.81909	1	0	0	1
-6.5035	-4.4164	0.36266	0	1	0	0	-0.0134
6.39946	-1.727	1	0	0	1	0.05179	-0.0735
0.043	-1	0	1	0	-0.0681	0.05621	-0.0167
0	1	0	2	0.0625	-0.0161	0.01503	0.01327
1	0	1	0.05621	-0.0838	0.04984	-0.0022	0.01586
1	1	-0.0503	-0.0387	-0.0496	0.07412	-0.0092	0.0221
0	-0.073	0.05961	-0.014	-0.0335	0.00767	-0.0607	0.01803

(c) Rounded stego-quantization left block

60.0234	-2.354	4.27138	0.15956	0	1	0	0
-7.5821	-3.8683	0.28948	0	0	1	1	0.02624
5.85113	-2.1627	0	-1	1	0	0.04771	0.02244
-0.5991	-1	0	0	0	-0.0013	-0.0709	-0.066
1	2	2	0	-0.2188	-0.0344	-0.0603	-0.0461
2	1	0	0.08253	0.04172	0.07793	0.03189	0.0266
0	0	0.03259	-0.0535	0.07038	0.0381	0.02187	0.00788
1	-0.1159	0.01402	-0.1027	-0.0338	-0.0537	-0.0142	-0.0297

(d) Rounded stego-quantization right block

60.3828	-3.6949	3.86056	0.81459	0.45313	-0.0014	0.00215	0.03523
-6.5007	-4.3926	0.37884	-0.2823	-0.0132	0.0314	-0.023	-0.0186
6.35525	-1.7201	-0.1324	-0.4665	-0.398	-0.0217	0.05488	-0.0754
0.03598	-1.0594	-0.3776	0.22114	-0.0303	-0.0699	0.0572	-0.0242
-0.2431	0.97101	0.36869	0.54354	0.06434	-0.0145	0.01213	0.01515
1.26201	-0.4304	-0.2273	0.05091	-0.0826	0.04929	-0.0017	0.01669
-0.3959	-0.2011	-0.0508	-0.0332	-0.0529	0.07057	-0.0073	0.02534
0.26733	-0.0781	0.06008	-0.014	-0.0306	0.007	-0.0567	0.01688

(e) Recovered-quantization left block  $sB_Q^{L'}$

60.0078	-2.3486	4.29448	0.14466	-0.1094	-0.3502	-0.1127	-0.0227
-7.5805	-3.8923	0.26868	-0.3992	0.07253	-0.0092	0.05305	0.02841
5.82497	-2.1482	-0.289	-0.6421	-0.1968	0.20772	0.04408	0.01172
-0.6546	-1.4682	-0.463	-0.045	-0.2702	0.00034	-0.0697	-0.0639
0.25694	1.11092	0.6711	0.32597	-0.2224	-0.0346	-0.0618	-0.0424
1.29987	-0.391	0.0269	0.07527	0.04371	0.07607	0.03026	0.02319
-0.3884	-0.2558	0.03579	-0.0527	0.07238	0.03969	0.02187	0.00415
0.17309	-0.1158	0.00816	-0.1078	-0.0385	-0.0544	-0.0167	-0.0293

(f) Recovered-quantization right block  $sB_Q^{R'}$

(g) Extracted secret bits  $s = 101001001010110110010001000111101$

Fig. 10 Example of recovering cover-image and extracting secret data

contains 21 different stereo-images and six pairs of stereo-images from dataset are shown in Fig. 11. In the experiment, the Baboon image, shown in Fig. 12, is treated as a secret data. All algorithms in this section are implemented in the MATLAB version 8.3 software running on an Intel® Core™ i5 processor 3.2GHz with 4GB RAM.

To evaluate the performance of data hiding schemes, two important factors: embedding capacity and visual quality are used. To estimate the performance of the embedding capacity, the embedding rate with the unit of bits per pixel (bpp) is used and that is calculated by Eq. (10):

$$bpp = \frac{\text{number of embedded bits}}{\text{number of pixels of cover image}} \tag{10}$$

To estimate the visual image quality, a peak-signal-to-noise (PSNR) ratio is used, the PSNR is calculated as follows:

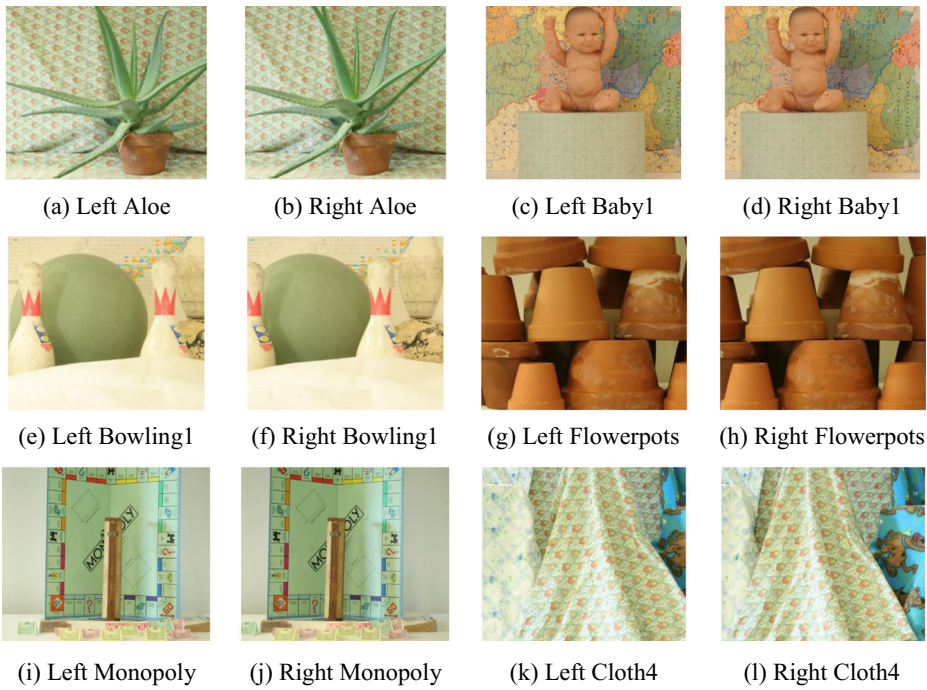


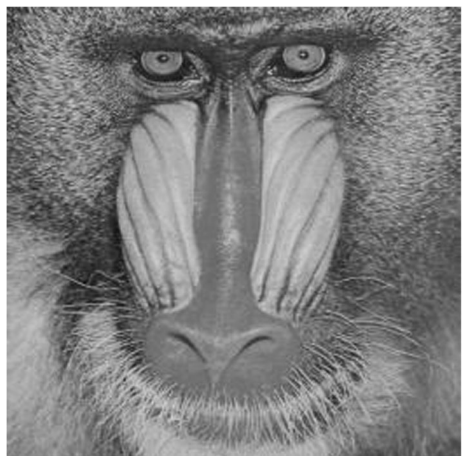
Fig. 11 Six pairs of stereo images in the dataset [24]

$$PSNR = 10 \log_{10} \frac{255^2}{MSE} \tag{11}$$

where *MSE* is the mean squared error representing the difference between the original image and stego-image and is defined as follows:

$$MSE = \frac{1}{M \times N} \sum_{i=1}^M \sum_{j=1}^N (x_{i,j} - x'_{i,j})^2 \tag{12}$$

Fig. 12 Baboon – Secret data



with  $M$  and  $N$  as the height and width of the cover image, respectively, and  $x_{i,j}$  and  $x'_{i,j}$  refer to the pixels located at the  $i$ th row and  $j$ th column of original image and stego-image, respectively.

In the proposed scheme, different values of quality factors ( $QF$ ) and the threshold  $T$ , i.e.,  $QF = 50, 60, 70, 75, 80,$  or  $90$  and  $T = 5, 10, 15, 20,$  or  $25$  are utilized for testing. Table 2, provided the visual quality and the embedding rate of the proposed scheme under different quality factors when threshold  $T$  is equal to 5. The table represents the results of performance in terms of visual quality (PSNR) and embedding rate (bpp) of the 21-stereo-image dataset. It is obvious that the lower the quality factor is, the higher the embedding capacity is achieved. Additionally, from the results, it can be seen that the proposed scheme maintains the good image quality, when the PSNR value is always greater than 32 dB.

Table 3. shows the performance of the proposed scheme, in terms of the visual image quality and embedding rate with  $QF = 75$  and under various values of the threshold  $T$ . As can be seen in Table 3, the larger threshold  $T$  is used, the higher embedding rate will be obtained while the lower visual quality will be. This is because when the threshold  $T$  is small, fewer similarity block pairs are found in the search phase, causing the low embedding rate. In contrast, when the threshold  $T$  becomes larger, the embedding capacity increases this is because the more similar block pairs are determined then more secret bits are embedded.

To further confirm the advantage of our scheme, we compared our scheme with the state-of-the-art scheme proposed by Yang and Chen [26] in terms of capacities and PSNRs. To accomplish this, the dataset mentioned above and the secret data bits generated from the Baboon image are used as input values of the proposed scheme and the scheme [26]. Table 4 shows the performance comparison of the proposed scheme and Yang et al.'s scheme for 21 stereo images when the quality factor  $QF = 75$  and different thresholds  $T$  are used. From Table 4, we can see that the average PSNR values and average embedding rates obtained by the proposed scheme are much larger than those of Yang et al.'s scheme. This is because most of QDCT coefficient pairs are

**Table 2** The PSNR and bpp of embedding rate of the proposed scheme under different values of  $QF$  and  $T = 5$

Images	$QF = 50$ PSNR	bpp	$QF = 60$ PSNR	bpp	$QF = 70$ PSNR	Bpp	$QF = 80$ PSNR	bpp	$QF = 90$ PSNR	bpp
Aloe	37.268	0.103	40.008	0.064	44.512	0.031	52.763	0.008	71.701	0.001
Baby1	34.391	0.288	36.027	0.241	38.808	0.175	44.290	0.089	57.776	0.013
Baby2	33.490	0.339	35.124	0.282	38.133	0.197	43.870	0.098	54.835	0.029
Baby3	34.102	0.316	35.852	0.259	38.898	0.180	44.146	0.092	58.227	0.010
Bowling1	33.101	0.429	34.308	0.395	36.360	0.346	40.257	0.260	50.289	0.103
Bowling2	34.788	0.272	36.257	0.238	38.732	0.185	43.589	0.108	57.862	0.012
Cloth1	38.332	0.074	41.059	0.045	45.100	0.022	52.810	0.006	69.762	0.000
Cloth2	39.264	0.093	41.893	0.062	46.317	0.031	53.121	0.011	72.031	0.000
Cloth3	37.372	0.129	39.934	0.082	44.458	0.037	52.303	0.009	69.852	0.001
Cloth4	39.743	0.074	42.346	0.050	47.155	0.023	55.695	0.007	Infinite	0.000
Flowerpots	35.049	0.280	36.765	0.231	39.579	0.170	44.447	0.103	55.048	0.029
Lampshade1	32.951	0.437	34.251	0.397	36.482	0.337	40.425	0.258	48.413	0.163
Lampshade2	32.963	0.468	34.310	0.420	36.625	0.348	40.893	0.237	49.459	0.116
Midd1	33.439	0.392	34.581	0.371	36.474	0.342	39.782	0.297	46.393	0.232
Midd2	33.455	0.407	34.619	0.384	36.510	0.352	39.909	0.292	46.925	0.210
Monopoly	36.545	0.203	38.312	0.164	40.967	0.124	45.027	0.085	53.423	0.042
Plastic	33.597	0.443	34.780	0.414	36.644	0.376	40.086	0.309	47.427	0.198
Rocks1	36.487	0.164	38.942	0.114	43.181	0.061	50.326	0.025	63.985	0.004
Rocks2	37.762	0.119	41.028	0.068	46.155	0.030	53.762	0.010	64.842	0.003
Wood1	33.181	0.407	34.588	0.350	37.265	0.250	43.305	0.103	59.586	0.007
Wood2	32.363	0.478	33.732	0.424	36.183	0.332	41.129	0.198	54.104	0.044



**Table 3** Stego-stereo image quality and embedding capacity of 21 images when  $QF = 75$

Images	T = 5 PSNR	bpp	T = 10 PSNR	bpp	T = 15 PSNR	bpp	T = 20 PSNR	bpp	T = 25 PSNR	bpp
Aloc	47.625	0.018	44.033	0.043	42.114	0.065	40.954	0.083	40.208	0.097
Baby1	40.883	0.137	39.098	0.209	38.336	0.247	37.873	0.274	37.480	0.295
Baby2	40.317	0.152	38.305	0.238	37.477	0.284	36.932	0.317	36.616	0.340
Baby3	40.925	0.141	39.070	0.218	38.156	0.265	37.564	0.302	37.221	0.326
Bowling1	37.812	0.315	37.154	0.370	36.795	0.402	36.570	0.421	36.398	0.435
Bowling2	40.539	0.155	39.212	0.211	38.638	0.241	38.265	0.261	38.008	0.278
Cloth1	48.120	0.013	45.111	0.027	43.173	0.042	41.978	0.055	41.037	0.068
Cloth2	48.987	0.021	45.883	0.043	43.673	0.068	42.618	0.086	41.623	0.105
Cloth3	47.639	0.021	43.847	0.054	41.883	0.084	40.784	0.111	40.018	0.132
Cloth4	50.378	0.015	46.616	0.034	44.449	0.053	43.342	0.066	42.729	0.074
Flowerpots	41.381	0.141	39.855	0.201	39.006	0.247	38.501	0.280	38.084	0.306
Lampshade1	38.041	0.303	37.135	0.366	36.684	0.402	36.457	0.426	36.300	0.443
Lampshade2	38.279	0.299	37.204	0.387	36.754	0.430	36.479	0.459	36.268	0.477
Midd1	37.799	0.325	37.331	0.357	37.117	0.375	36.919	0.389	36.809	0.399
Midd2	37.903	0.325	37.357	0.368	37.115	0.389	36.929	0.403	36.794	0.416
Monopoly	42.645	0.106	41.411	0.142	40.625	0.173	40.010	0.201	39.529	0.224
Plastic	38.009	0.348	37.472	0.397	37.249	0.422	37.078	0.440	36.903	0.454
Rocks1	46.118	0.042	42.638	0.084	40.991	0.118	39.867	0.147	39.156	0.172
Rocks2	49.306	0.019	45.270	0.044	42.753	0.076	41.083	0.108	40.049	0.135
Wood1	39.497	0.186	37.629	0.297	36.999	0.352	36.651	0.383	36.475	0.404
Wood2	38.109	0.273	36.720	0.375	36.167	0.427	35.855	0.457	35.702	0.476

concentrated on one quarter of the 2D histogram so only the corresponding corner of histogram is used for embedding data. Therefore, QDCT coefficients in one suitable corner of histogram are modified while three other histogram corners remain unchanged, instead of modifying all the different values in the 1D histogram for embedding data as was done in Yang and Chen’s scheme. Moreover, to expand the embedding area in the proposed scheme, other pairs, i.e. (0,1) or (1, 0), in the selected histogram, are used to embed one more secret bit. Referring to Fig. 13, it is clear that the proposed scheme achieved higher performance in terms of embedding capacity and image quality than that of the scheme [26], when twelve tested images are used with the threshold  $T = 20$  and  $QF = 75$ . Figure 13 shows that the proposed scheme is always superior to Yang and Chen’s scheme in terms of embedding capacity and visual image quality. Specifically, the embedding capacity of the previous scheme [26] equaled only approximately half that of the proposed scheme.

The graph in Fig. 14 shows the highest embedding capacity (bits) of the proposed scheme and Yang and Chen’s scheme with the threshold  $T = 30$  and  $QF = 75$  for 21 stereo images when the PSNR is set to 45 (dB). The figure indicates that capacities of the proposed scheme are significantly

**Table 4** Comparison between our scheme and Yang and Chen’s scheme with an average PSNR and embedding rate of 21 stego-images when quality factor  $QF = 75$

T	Yang and Chen’s scheme		Our scheme	bpp
	PSNR	bpp		
5	42.354	0.131	42.396	0.160
10	40.324	0.176	40.398	0.213
15	39.258	0.205	39.341	0.246
20	38.598	0.227	38.700	0.270
25	38.140	0.243	38.258	0.288
30	37.808	0.256	37.929	0.303

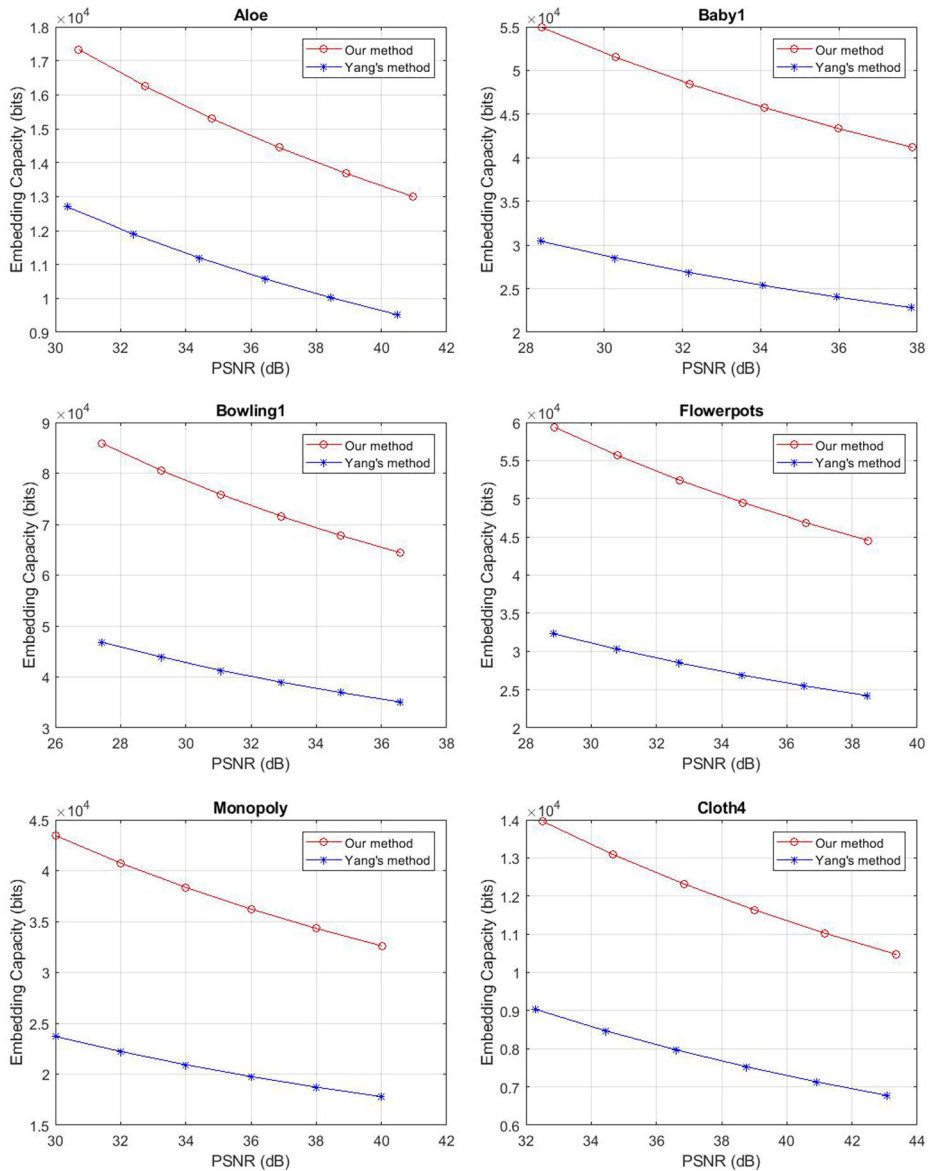


Fig. 13 Performance comparison between the proposed scheme and Yang et al.'s scheme with  $T = 20$ ,  $QF = 75$

higher than that Yang and Chen's scheme in all different images. Specifically, take Lampshade2 image as example, the scheme can embed 62,814 bits, while only 34,453 bits are embedded by Yang and Chen's scheme. In addition, the embedding capacity in bits increases dramatically in the proposed scheme, up to more than 82%. Take Cloth1 image as another example, the results obtained by two schemes are both limited, this is because the Cloth1 image is one of complicated images, therefore, it is difficult to search the match similar blocks in the left and right image. As a consequence, the low embedding capacity will be obtained. However, the embedding capacity of the proposed scheme is also better than that of the Yang and Chen's scheme.

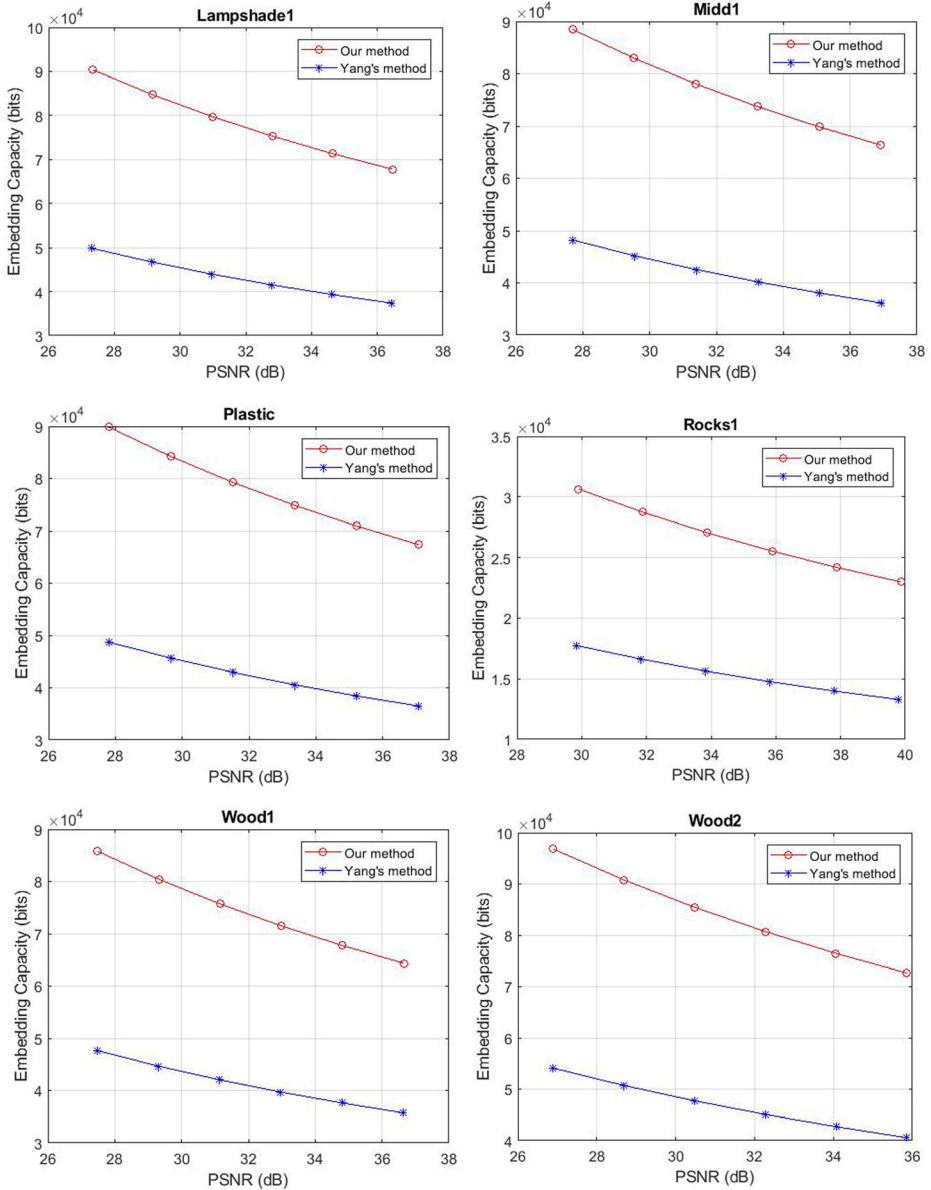
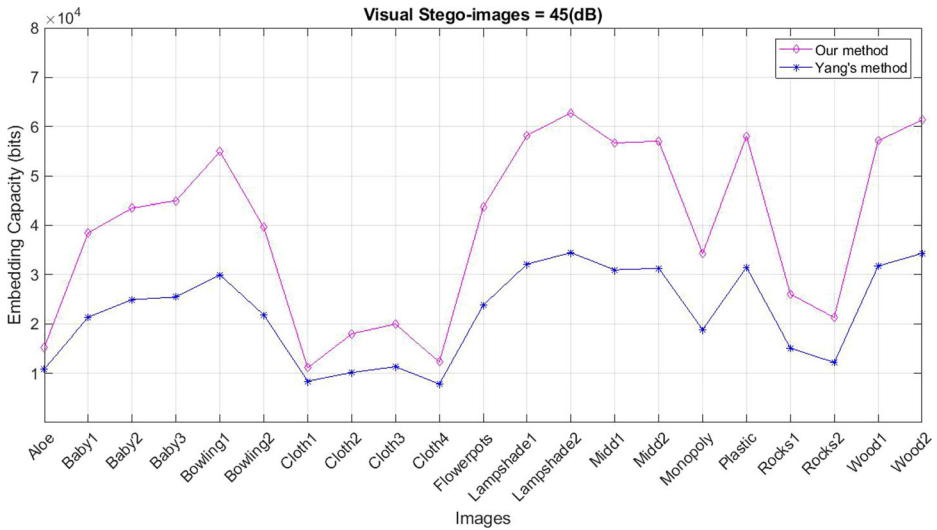


Fig. 13 (continued)

In Table 5, we compared the proposed scheme's performance with those of three other existing frequency based hiding schemes [5, 14, 26]. Table 5 demonstrated that the embedding rate of the Yang and Chen's scheme [26] is significantly higher than those of the two other schemes [5, 14]. However, that the embedding rate of the Yang and Chen's scheme (0.131 bpp) is still lower than that of the proposed scheme (0.160 bpp). The main reason is that Yang and Chen's scheme has applied 1D histogram shifting to embed approximately 1.6 secret bits



**Fig. 14** Performance comparison between the proposed scheme with Yang and Chen’s scheme on the dataset with threshold  $T = 30$ ,  $QF = 75$

into a pair of QDCT coefficients in stereo images, when the different value of these coefficients is equal to zero. However, most of the QDCT coefficient pairs in the embedding area of the left and the right images have the values of (0, 0). Therefore, the embedding capacity of Yang and Chen’s scheme is limited by the number of pair (0, 0). In contrast, the 2D histogram shifting is applied in the proposed scheme to further improve embedding rate. By doing so, for each pair with the values of (0, 0), one or two secret bits are embedded in the proposed scheme. As a result, the embedding capacity is increased. Furthermore, the embedding area in the proposed scheme is expanded, meaning some other pairs, i.e. (0,1) or (1, 0), in the selected histogram corner, are used to embed one more secret bit. In addition, by using the 2D histogram, only one histogram corner is selected and modified for embedding data, thus the good stego-stereo image quality is guaranteed. In Table 5, the proposed scheme provides satisfactory image quality, with the PSNR with  $QF = 75$  and  $T = 5$  always being greater than 42 dB, a result that is considerably better than those of Yang and Chen’s scheme [26] and other two schemes [5, 14].

### 5 Conclusion

In this paper, we proposed a novel reversible data hiding scheme for stereo images. The proposed scheme, 2D histogram based on the QDCT coefficient pairs is plotted to hide secret

**Table 5** Performance comparison between our scheme with some existing schemes with  $T = 5$ ,  $QF = 75$

Schemes	Average PSNR (dB)	Average embedding rate (bpp)	Domain	Reversibility
Parah et al.’s scheme [14]	41.48	0.015	DCT	No
Guo et al.’s scheme [5]	39.82	0.015	DWT + DCT	No
Yang and Chen’s scheme	42.35	0.131	DCT	Yes
Our scheme	42.40	0.160	DCT	Yes

data bits. The proposed solution offers reversibility and high embedding capacity while maintaining acceptable quality of stereo-images. The experimental results prove that, our solution outperforms Yang et al.'s scheme in data hiding capacity and stego-stereo images quality. In addition, the proposed scheme is also suitable for embedding secret message on stereo images for medical, military or forensic applications since the scheme restore perfectly cover- stereo image from stego-stereo image with lossless information.

**Acknowledgements** This research is funded by Vietnam National Foundation for Science and Technology Development (NAFOSTED) under grant number 102.01-2016.06

## References

- Campisi P (2008) Object-oriented stereo-image digital watermarking. *J Electron Imaging* 17(4):043024–043024-5
- Celik MU, Sharma G, Tekalp AM, Saber E (2005) Lossless generalized-LSB data embedding. *IEEE Trans Image Process* 14(2):253–266
- Chang C-C, Chen T-S, Chung L-Z (2002) A steganographic scheme based upon JPEG and quantization table modification. *Inf Sci* 141(1–2):123–138
- Chang C-C, Hsiao J-Y, Chan C-S (Jul. 2003) Finding optimal least-significant-bit substitution in image hiding by dynamic programming strategy. *Pattern Recogn* 36(7):1583–1595
- Guo J, Zheng P, Huang J (2015) Secure Watermarking Scheme against Watermark Attacks in the Encrypted Domain. *J Vis Commun Image R* 30:125–135
- Huang F, Qu X, Kim HJ, Huang J (2016) Reversible Data Hiding in JPEG Images. *IEEE Trans Circuits Syst Video Technol* 26(9):1610–1621
- Kumar R, Chand S (2016) A reversible high capacity data hiding scheme using pixel value adjusting feature. *Multimed. Tools Appl.* 75(1):241–259
- Lin Y-K (2012) High capacity reversible data hiding scheme based upon discrete cosine transformation. *J Syst Softw* 85(10):2395–2404
- Luo T, Jiang G, Wang X, Yu M, Shao F, Peng Z (2014) Stereo image watermarking scheme for authentication with self-recovery capability using inter-view reference sharing. *Multimed. Tools Appl.* 73(3):1077–1102
- Ni Z, Shi Y-Q, Ansari N, Su W (2006) Reversible data hiding. *IEEE Trans Circuits Syst Video Technol* 16(3):354–362
- Nikolaidis A (2015) Reversible data hiding in JPEG images utilising zero quantised coefficients. *IET Image Process* 9(7):560–568
- S. A. Parah, J. A. Akhoun, J. A. Sheikh, N. A. Loan, and G. M. Bhat, “A high capacity data hiding scheme based on edge detection and even-odd plane separation,” in *2015 Annual IEEE India Conference (INDICON)*, 2015, pp. 1–5
- S. A. Parah, F. Ahad, J. A. Sheikh, and G. M. Bhat, “On the realization of robust watermarking system for medical images,” in *2015 Annual IEEE India Conference (INDICON)*, 2015, pp. 1–5
- Parah SA, Sheikh JA, Loan NA, Bhat GM (2016) Robust and blind watermarking technique in DCT domain using inter-block coefficient differencing. *Digit Signal Process* 53:11–24
- Parah SA, Sheikh JA, Assad UI, Bhat GM (2017) Realisation and robustness evaluation of a blind spatial domain watermarking technique. *Int J Electron* 104(4):659–672
- Parah SA, Ahad F, Sheikh JA, Loan NA, Bhat GM (2017) A New Reversible and high capacity data hiding technique for E-healthcare applications. *Multimed. Tools Appl.* 76(3):3943–3975
- Parah SA, Sheikh JA, Ahad F, Loan NA, Bhat GM (2017) Information hiding in medical images: a robust medical image watermarking system for E-healthcare. *Multimed. Tools Appl.* 76(8):10599–10633
- Parah SA, Sheikh JA, Akhoun JA, Loan NA, Bhat GM (2018) Information hiding in edges: A high capacity information hiding technique using hybrid edge detection. *Multimed. Tools Appl.* 77(1):185–207
- F. PUB, *Data Encryption Standard (DES)*. 1999
- F. PUB, *Advanced Encryption Standard (AES)*. 2011
- Rivest RL, Shamir A, Adleman L (1978) A Scheme for Obtaining Digital Signatures and Public-key Cryptosystems. *Commun ACM* 21(2):120–126

22. J. Shade, S. Gortler, L. He, R. Szeliski (1998) “Layered Depth Images,” in *Proceedings of the 25th Annual Conference on Computer Graphics and Interactive Techniques*, New York, NY, USA, pp. 231–242
23. Tian J (2003) Reversible data embedding using a difference expansion. *IEEE Trans. Circuits Syst. Video Technol.* 13(8):890–896
24. “vision.middlebury.edu/stereo/data.” [Online]. Available: <http://vision.middlebury.edu/stereo/data/>. [Accessed: 31-Dec-2016]
25. Wang K, Lu Z-M, Hu Y-J (2013) A high capacity lossless data hiding scheme for JPEG images. *J Syst Softw* 86(7):1965–1975
26. Yang W-C, Chen L-H (2015) Reversible DCT-based data hiding in stereo images. *Multimed Tools Appl* 74(17):7181–7193



**Phuoc-Hung Vo** received the B.S. degree in information technology from Can Tho University, Can Tho City, Vietnam, in 1996. From October 1996 he has been lecturer of Travinh Continuous Training Center, Travinh Community College and then Tra Vinh University. In 2011, he received M.Sc degree in computer science from Feng Chia University, Taichung, Taiwan. Currently, he is pursuing Ph. D. degree in Cantho University, Vietnam. His current research interests are watermarking, data hiding, information security.



**Thai-Son Nguyen** received the bachelor's degree in information technology from the Open University, HCM city, Vietnam, in 2005. From December 2006, he has been lecturer of Tra Vinh University, Tra Vinh, Vietnam. In 2011 and 2015, he received M.S. degree and Ph.D. degree with the Department of Information Engineering and Computer Science, Feng Chia University, Taichung, Taiwan, respectively. He is currently Vice Dean of the School of Engineering and Technology, Tra Vinh University, Vietnam. His current research interests, including watermarking, data hiding, image and signal processing, multimedia security, information security.



**Van-Thanh Huynh** received the bachelor's degree in information technology from the Can Tho University, Can Tho city, Vietnam, in 2005. From December 2005, he has been lecturer of Tra Vinh University, Tra Vinh, Vietnam. In 2017, he received M.S. degree in information technology from the Department of Information Science and Engineering, Information Technology University, Ho Chi Minh city, Vietnam. His current research interests, including watermarking, steganography, image processing, information security, computer networking.



**Thanh-Nghi Do** is currently head of the computer networks department, associate professor at the College of Information Technology, Cantho University, Vietnam. He is also associate researcher at the UMMISCO 209 (IRD/UPMC), Sorbonne University, Pierre and Marie Curie University - Paris 6, France. He received the M.S. and Ph.D. degrees in Computer Science from the University of Nantes, in 2002 and 2004, respectively. His research interests include data mining with support vector machine, kernel-based methods, decision tree algorithms, ensemble-based learning, information visualization. He has served on the program committees of international conferences and a reviewer for the journals in his fields.